# Pressure sensitivity for head, face and neck in relation to soft tissue

Yang, Wenxiu; He, Renke; Goossens, Richard; Huysmans, Toon

**DOI**
10.1016/j.apergo.2022.103916

**Publication date**
2023

**Document Version**
Final published version

**Published in**
Applied Ergonomics

Applied Ergonomics 106 (2023) 103916

Contents lists available at ScienceDirect

Applied Ergonomics

journal homepage: www.elsevier.com/locate/apergo

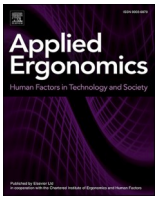

# Pressure sensitivity for head, face and neck in relation to soft tissue

Wenxiu Yang [a], Renke He [a,*], Richard Goossens [b], Toon Huysmans [b]

[a] School of Design Hunan University, Taozi Road, Changsha, 410000, China
[b] The Faculty of Industrial Design Engineering, Delft University of Technology, 2628CE, Delft, the Netherlands

ARTICLE INFO

*Keywords:*
Pressure discomfort
CT data
Product design

ABSTRACT

Pressure sensitivity research on the head, face, and neck is critical to develop ways to reduce discomfort caused by pressure in head-related products. The aim of this paper is to provide information for designers to be able to reduce the pressure discomfort by studying the relation between pressure sensitivity and soft tissue in the head, face and neck. We collected pressure discomfort threshold (PDT) and pressure pain threshold (PPT) from 119 landmarks (unilateral) for 36 Chinese subjects. Moreover, soft tissue thickness data on the head, face and neck regions of 50 Chinese people was obtained through CT scanning while tissue deformation data under the PDT and PPT states was obtained from literature. The results of the three-elements correlation analysis revealed that soft tissue thickness is positively correlated with deformation but not an important factor in pressure sensitivity. Our high-precision pressure sensitivity maps confirm earlier findings of more rough pressure sensitivity studies, while also revealing additional fine scale sensitivity differences. Finally, based on the findings, a high-precision "recommended map" of the optimal stress-bearing area of the head, face and neck was generated.

## 1. Introduction

In order for wearable products to achieve their basic functions they need to partially or completely cover the relevant body part and be seamlessly fitted to it. But excessive pressure during this process can cause discomfort or even pain (Shah et al., 2017). Therefore, investigations of the pressure sensitivity of various body parts and the creation of high-precision pressure maps are critical for reducing the pressure discomfort of wearable products. Many previous studies have investigated this area and measured the pressure sensitivity of various body parts, particularly the PPT (Pressure pain threshold) and PDT (Pressure discomfort threshold). For instance, the feet (Buso and Shitoot, 2019; Dueñas et al., 2021; Weerasinghe et al., 2017; Wiggermann and Keyserling, 2015; Xiong et al., 2011, 2013), the hands and elbows (Brigida et al., 2021; Le Johansson et al., 1999; Nasir et al., 2019), the back and buttock (Vink and Lips, 2017). This paper will concentrate on the head, face, and neck.

Pressure sensitivity studies, particularly pressure pain thresholds studies, have been commonly used in the medical field in the past. For example, the measurement of PPT at a specific position of the cervical spine (Binderup et al., 2010; Prushansky et al., 2004; Chung et al., 1992; Ferreira et al., 2020), and at different landmarks of the head and face (Fredriksson et al., 2000; Álvarez-Méndez et al., 2017; Waller et al., 2016), or a comparative study of pressure pain thresholds between healthy people and patients with a particular type of medical condition, such as patients with a headache (Castien et al., 2021; Sand et al., 1997; Barón et al., 2017). But few studies on pressure sensitivity in the head region include PDT tests. Because of the greater concern with discomfort, PPT studies alone are insufficient. In the area of discomfort, Broekhuizen et al. (2018) developed a European head pressure sensitivity map by measuring 19 Europeans head PDT and PPT for helmet design. Shah et al. (Shah and Luximon, 2021) gathered PDTs and PPTs on the head regions for 218 Chinese participants and created pressure sensitivity maps, laying the groundwork for designing head-related products for Chinese users. However, in the above studies, the pressure-sensitivity maps concentrated on contrasts between large head and facial regions, such as the higher pressure sensitivity of the face and nose. Moreover, the head and face structures are complex, as are the types and structures of head-related products. For example, mask straps and the nose clips of glasses and goggles involve localized areas of the head and face, and these small areas are critical for affixing or positioning load-bearing structures for products. Therefore, to reduce the pressure discomfort of head-related products, such as in selecting contact and weight-bearing positions involving small areas, it is essential to have high-precision pressure sensitivity maps of the head, face, and neck.

In general, the sensation of pressure is due to the soft tissue of the

* Corresponding author.
*E-mail address:* renke0319@126.com (R. He).

https://doi.org/10.1016/j.apergo.2022.103916
Received 19 June 2022; Received in revised form 24 August 2022; Accepted 29 September 2022
Available online 5 October 2022

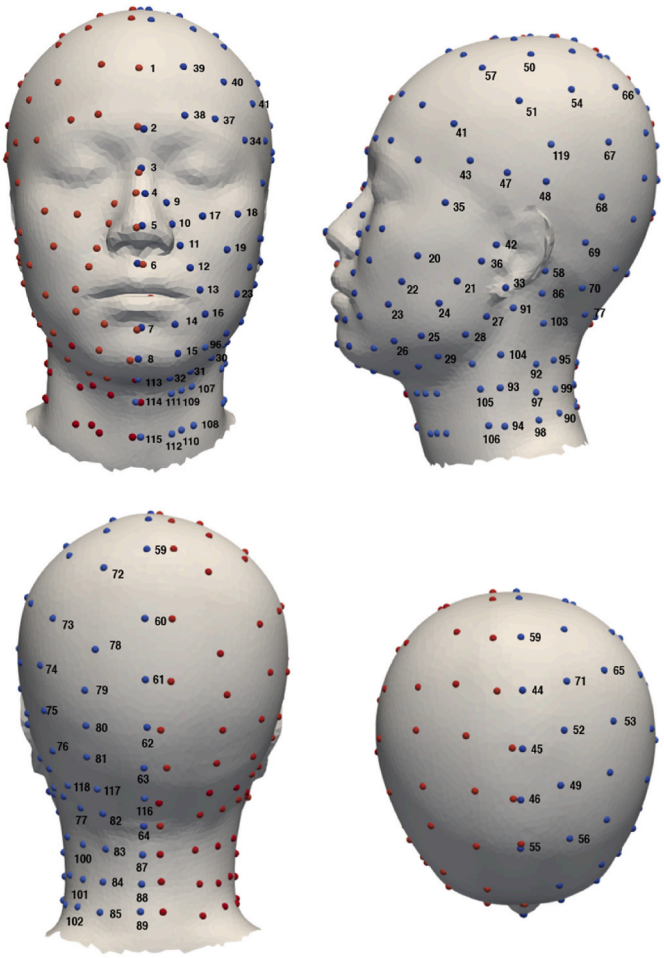

**Fig. 1.** Landmarks displayed on average head and mirrored from left (blue) to right (red) side. (For interpretation of the references to colour in this figure legend, the reader is referred to the Web version of this article.)

corresponding body part being deformed due to the forces generated by the product such as pressure, tension, friction. Therefore, biomechanical studies on the soft tissues of the head and face are crucial for pressure sensitivity, especially regarding studies on soft tissue thickness, since the thickness of the soft tissue affects the degree of deformation of the soft tissue. A large number of studies have measured the soft tissue thickness of the head and face among the existing facial soft tissue measurement studies. The facial soft tissue thickness data of Brazilian (Tedeschi-Oliveira et al., 2009) , Indian (Sahni et al., 2008), Turkish (Bulut et al., 2014), Chinese (Chen et al., 2011; He et al., 2021), South-Korean (Cha, 2013) and Indonesian (Sarilita et al., 2020) populations, have been collected and analyzed. However, these studies only measure the thickness of soft tissue at a limited number of landmarks in the craniofacial region. It is difficult to obtain accurate soft tissue thickness data of the head and face with a limited number of landmarks. Furthermore, the soft tissue thickness data obtained in the preceding studies are primarily presented in the form of data tables, which cannot directly display the thickness of the soft tissue of the head and face, nor can it be effectively applied to the head and face research related to the design of head-related products.

Facial soft tissue is typically measured in facial restoration. In forensics and archaeology, reconstruction of facial soft tissues is essential for accurate identification (De Greef and Willems, 2005). The needle depth probing method is used on cadavers in traditional soft tissue thickness measurement (Chopra et al., 2015). However, limitations of the corpse and the measurement method can considerably affect the accuracy of the results. Medical imaging technologies such as magnetic resonance imaging (MRI) (Lacko et al., 2015) and CT can effectively solve this problem.

Furthermore, and more importantly, previous studies in ergonomics on pressure sensitivity, soft tissue thickness, and soft tissue deformation are relatively independent. For example, Shah et al. (2022) also measured the degree of soft tissue deformation of 18 landmarks on the head and face of Chinese people in PDT and PPT states. However, they do not report on the relation among the three elements and they did not report the tissue thickness.

Based on the knowledge gap mentioned above, the aim of this paper is to provide information for designers to be able to reduce the pressure discomfort of head-related products by studying the relation between pressure sensitivity and soft tissue in the head, face and neck. In order to answer this aim, this paper created high-precision Chinese PDT and PPT maps, as well as high-precision Chinese soft tissue thickness maps using CT data. In addition, this study answers the question, "What is the relation between pressure sensitivity, soft tissue thickness, and soft tissue deformation in the head region?". Further, a "recommended map" of the optimal stress-bearing area of the head, face and neck was generated based on the above conclusions.

## 2. Methodology

The datasets in this paper are divided into three parts: PDT and PPT values, soft tissue thickness data, and soft tissue deformation data. In addition to the soft tissue deformation data from other literature, in this study we collected new data for the pressure threshold (PDT and PPT) and soft tissue thickness data. However, this section describes them separately because the pressure threshold and soft tissue thickness data were obtained through different experiments.

### 2.1. Participants

For pressure threshold (PDT and PPT value), subjects were recruited by posting advertisements in the university. Thirty-six healthy Chinese (20 males, 16 females) aged 18–30 were selected to participate in the pressure sensitivity experiment. Subjects with a history of facial fractures, swelling, deformity, image distortion, and pathological asymmetry, or any other pathology that might affect normal craniofacial features prior to measurement were barred from participating in the study. In addition, participants with a chronic or acute physical or mental health history or taken non-regular medication in two weeks before the experiment were also excluded. All individuals reported normal cardiovascular parameters, normal sensations, and healthy skin on their upper limbs and head/face. Before the experiment, all participants gave informed consent and required to wear low-necked clothes, and not to cover the neck and upper parts.

Moreover, in order to collect soft tissue thickness data, based on CT data collected in a previous study (He et al., 2021), 50 subjects (24 males and 26 females) were chosen for analysis in this study. All of the participants were Han Chinese from China's Hunan Province. Between the ages of 18 and 35. Subjects with a history of facial fractures, swelling, deformity, image distortion, and pathological asymmetry, or any other pathology that might affect normal craniofacial features prior to measurement were barred from participating in the study. All subjects gave informed consent.

### 2.2. Landmarks selection

Since there is no unified standard for selecting craniofacial landmarks and deciding regional divisions in anatomy (Stephan and Simpson, 2008). In order to make the Chinese pressure sensitive map more accurate than the previous studies, a high density selection of landmarks is needed which also covers beyond anatomical and morphological landmarks. Therefore, this study first takes anatomical landmarks as the basic landmarks (Stephan and Simpson, 2008), connects the anatomical

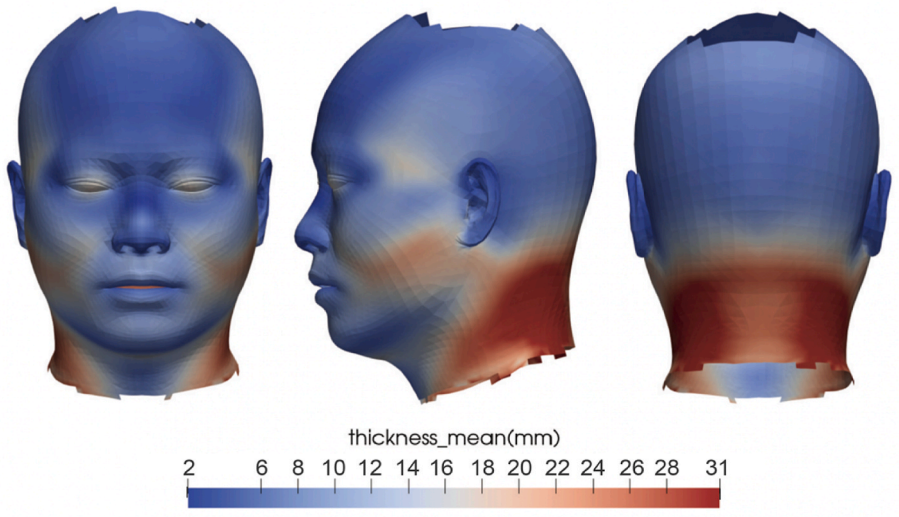


**Fig. 2.** Chinese soft tissue thickness map (unisex).

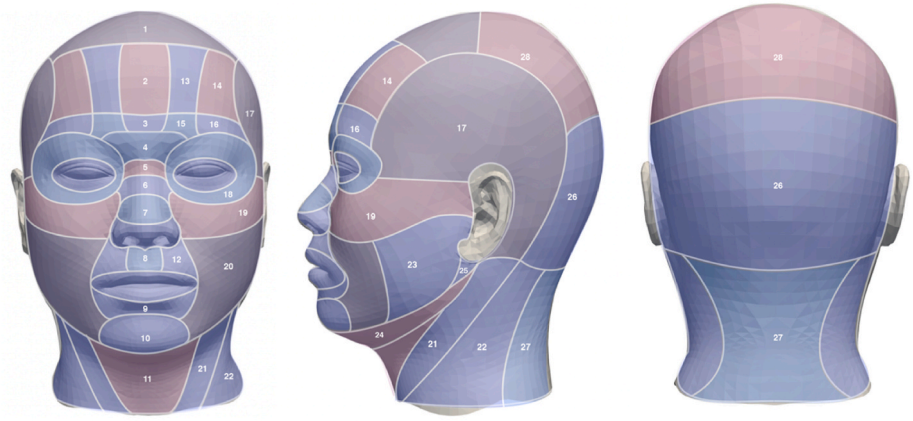

**Fig. 3.** 28 regions for head, face and neck.

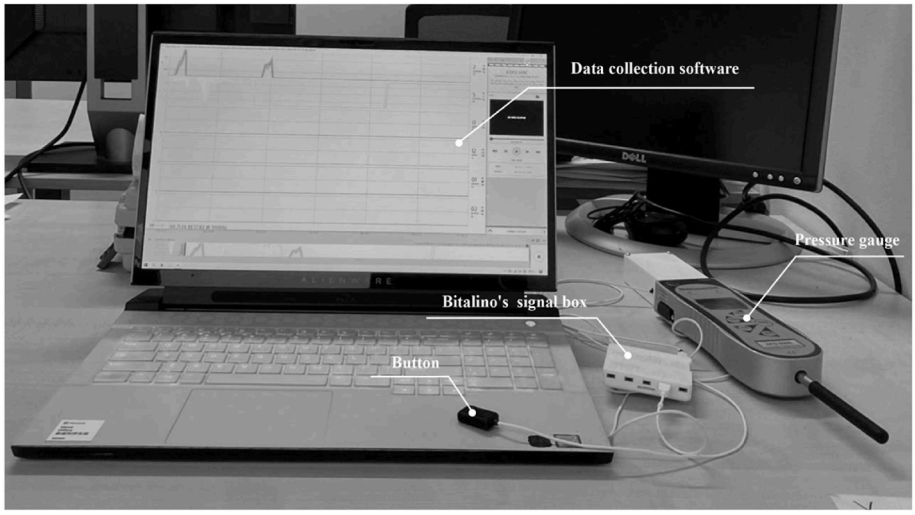


**Fig. 4.** Data collection system.

landmarks, and then distributes lines at equal distances, with each distance node representing a landmark. Finally, 119 high-density landmarks (unilateral) were chosen to cover the majority of the head, face, and neck (Fig. 1).

In addition, in order to ensure the accuracy of the soft tissue thickness map, when calculating the soft tissue thickness, the overall soft

**Fig. 5.** 3D scanning posture (left) and the specific posture of applied pressure (right).

tissue thickness of the entire head region was exported based on CT data rather than selecting a limited number of landmarks (Wenxiu Yang et al., 2022). Finally, the Chinese soft tissue thickness map with high precision was created (Fig. 2). However, to facilitate the comparative analysis of the data and make the visualization of the soft tissue thickness map and the pressure sensitivity map higher, this study divided the head, face, and neck into multiple regions.

The current study aimed to develop ways to reduce the pressure discomfort of head-related products by studying the relation between pressure sensitivity and soft tissue in the head, face and neck. Therefore, anatomical structure was used as the major standard for structural division in this study, while the soft tissue thickness map and pressure sensitivity map were used as sub-regional division criteria. After division, the scalp, face, and neck were further divided into 28 areas (unilateral) (Fig. 3). Based on the structure of the skull, the scalp was divided along the frontal, parietal, temporal, and occipital bones; the soft tissue thickness of these parts was also found to be consistent. The neck structure is complex, having numerous muscles, a vertebral structure in the back, and the trachea and esophagus in the front. Therefore, the regional division of the neck was based on the structure of the neck muscles, and the sub-regional division criteria was based on the soft tissue thickness map and the pressure sensitivity map. Moreover, the face exhibited the most intricate structure, with multiple organs. Chopra et al. (2015)divided the face into multiple regions and measured soft tissue thickness, but the results revealed multiple adjacent regions with similar soft tissue thickness that could be merged. As a result, the current was based on Chopra's face division method and incorporated several regions via the soft tissue thickness map and the pressure sensitivity map. Finally, the head, face, and neck were divided into 28 regions in this paper (unilateral). From 28 regions, 28 landmarks (unilateral) with anatomical significance were chosen for data extraction.

### 2.3. Equipment and procedure

Pressure probes are widely used to measure local PPT and PDT (Jayaseelan et al., 2021; Spano et al., 2021; Kosek et al., 1993). In this experiment, an Advanced Force Gauge (AFG) meter (Mecmesin AFG 500N) with a flat tip with diameter of 10 mm was used to apply pressure. To accurately record the applied pressure, the pressure gauge was linked to Bitalino's (Páris et al., 2017) signal box and supporting data collection

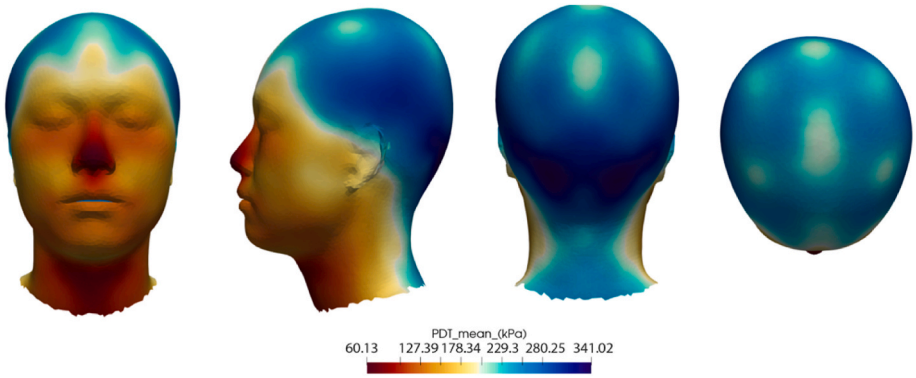


**Fig. 6.** PDT sensitivity map for Chinese (unisex).

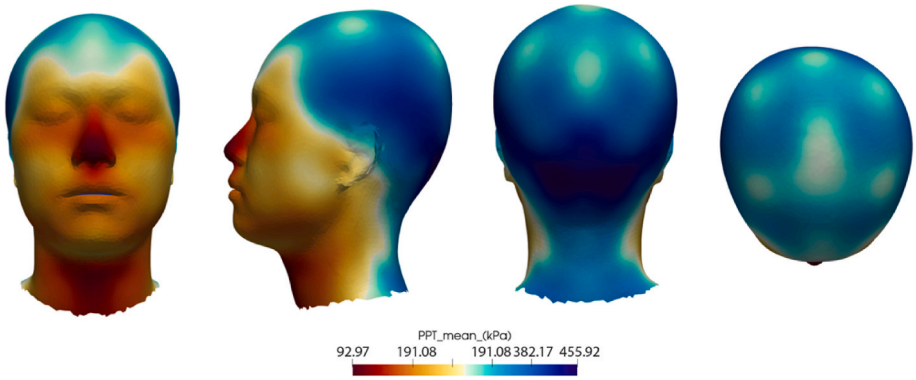


**Fig. 7.** PPT sensitivity map for Chinese (unisex).

**Table 4**
Pressure sensitivity and soft tissue thickness data for female and male.

| No. | Female | | | Male | | |
|---|---|---|---|---|---|---|
| | Pressure sensitivity (kPa) | | Soft tissue thickness (mm) | Pressure sensitivity (kPa) | | Soft tissue thickness (mm) |
| | PDT mean | PPT mean | Mean | PDT mean | PPT mean | Mean |
| 1 | 190.38 | 244.9 | 4.3 | 235.67 | 323.81 | 4.98 |
| 2 | 191.46 | 258.41 | 4.04 | 257.88 | 359.55 | 4.53 |
| 3 | 154.39 | 203.38 | 5.11 | 185.91 | 269.82 | 5.55 |
| 4 | 126.55 | 175.1 | 5.93 | 151.14 | 206.72 | 6.17 |
| 5 | 104.71 | 146.82 | 5.12 | 120.38 | 163.61 | 5.94 |
| 6 | 84.65 | 117.45 | 2.43 | 101.67 | 140.84 | 2.67 |
| 7 | 54.01 | 82.55 | 7.06 | 67.6 | 105.41 | 8.22 |
| 8 | 87.77 | 128.85 | 9.61 | 106.45 | 154.7 | 11.28 |
| 9 | 116.11 | 159.75 | 8.98 | 143.79 | 216.8 | 9.93 |
| 10 | 116.5 | 171.46 | 9.86 | 155.1 | 244.9 | 9.93 |
| 11 | 67.07 | 96.05 | 9.19 | 86.86 | 133.04 | 7.75 |
| 12 | 131.72 | 187.83 | 8.78 | 177.31 | 247.69 | 10.63 |
| 13 | 244.2 | 329.36 | 3.84 | 279.06 | 372.13 | 4.34 |
| 14 | 216.94 | 291.08 | 3.52 | 298.96 | 382.25 | 4.05 |
| 15 | 176.37 | 245.67 | 5.26 | 213.69 | 306.21 | 5.51 |
| 16 | 151.72 | 199.87 | 4.6 | 204.86 | 279.06 | 5.47 |
| 17 | 250.32 | 3347.64 | 10.98 | 309.71 | 429.54 | 13.19 |
| 18 | 100 | 151.21 | 7.49 | 146.66 | 211.78 | 7.64 |
| 19 | 116.75 | 154.9 | 11.22 | 146.02 | 223.89 | 10.54 |
| 20 | 98.66 | 155.41 | 17.66 | 152.71 | 222.53 | 18.89 |
| 21 | 90 | 130.51 | 20.69 | 120.78 | 179.78 | 22.72 |
| 22 | 110.51 | 152.42 | 28.13 | 144.9 | 202.15 | 32.42 |
| 23 | 114.78 | 167.26 | 21.99 | 169.75 | 234.32 | 22.76 |
| 24 | 108.41 | 155.99 | 6.75 | 169.27 | 263.69 | 7.92 |
| 25 | 121.78 | 174.08 | 17.94 | 161.78 | 222.93 | 19.69 |
| 26 | 270.13 | 364.01 | 6.38 | 323.49 | 471.18 | 7.07 |
| 27 | 196.43 | 278.47 | 21.68 | 323.81 | 477.71 | 29.22 |
| 28 | 201.66 | 264.39 | 7.87 | 220.54 | 321.34 | 8.76 |

software (OpenSignals) to form a data collection system (Fig. 4). Participants were then given a button linked to this system. The researchers applied continuous pressure with a pressure gauge. When participants felt discomfort or pain, they were required to press buttons, and the time of initial discomfort and pain force values were recorded into the program and used for subsequent calculations.

The experiment process was mainly divided into three stages: First, the preparation stage. At this stage, basic information such as age, gender, height, and weight of the subjects was collected through questionnaires. Following that, subjects were required to wear a hair cap to straighten their hair. Female subjects with long hair were requested to tie it into a bun and fasten it behind their right ear. After initial preparation, researchers applied circular self-adhesive patches with landmark numbers to the subjects' heads, faces, and necks.

The second stage was the 3D scanning stage. Participants who completed the first stage were asked to sit on a turntable that rotated at a constant speed to collect 3D data of the head, face, and neck (Fig. 5). The third stage was the pressure application stage. During this phase, an experienced researcher visited all landmarks in random order and increased pressure with a rate between 30 and 40 kPa/s. When the subjects began to feel discomfort, they were asked to press an electronic button that recorded the PDT of specific landmarks. After this, the researcher would continue to apply increasing pressure, and the subjects were instructed to press the button again when they began to feel pain, to record the PPT of the landmarks and the stopping of pressure application. Each point was measured three times (for both PDT and PPT) per participant to measure the pressure threshold accurately (Shah and Luximon, 2021). The Ethics Committee approved this study at the Delft University of Technology (No.1975).

### 2.4. Data analysis

For the pressure sensitivity experiment, since the force value collected by OpenSignals is in volts (V), the signal was requested to be imported into Matlab for unit conversion. After that, SPSS software Ver. 25.0 (SPSS Inc., Chicago, USA) was used for data analysis. Descriptive statistics and difference analyses were performed for 119 landmarks from the PDT and PPT perspectives. The general descriptive statistics are expressed as the mean and standard deviation. The paired-sample *t*-test was adopted to compare the differences, and $P < 0.05$ was considered statistically significant. In addition, from 28 regions, 28 landmarks with anatomical significance were chosen for data extraction, including soft tissue thickness data and the corresponding pressure discomfort and pressure pain thresholds. Descriptive statistics were carried out in each landmark. The general descriptive statistics were expressed as the mean and the Pearson correlation coefficient was used for correlation analysis.

## 3. Results

The results of this paper were statistically described and analyzed from three parts: pressure threshold (PDT and PPT), comparison of pressure threshold and soft tissue thickness, and comparison among pressure threshold, soft tissue thickness, and soft tissue deformation.

Firstly, the PDT and PPT values of 119 landmarks for all participants

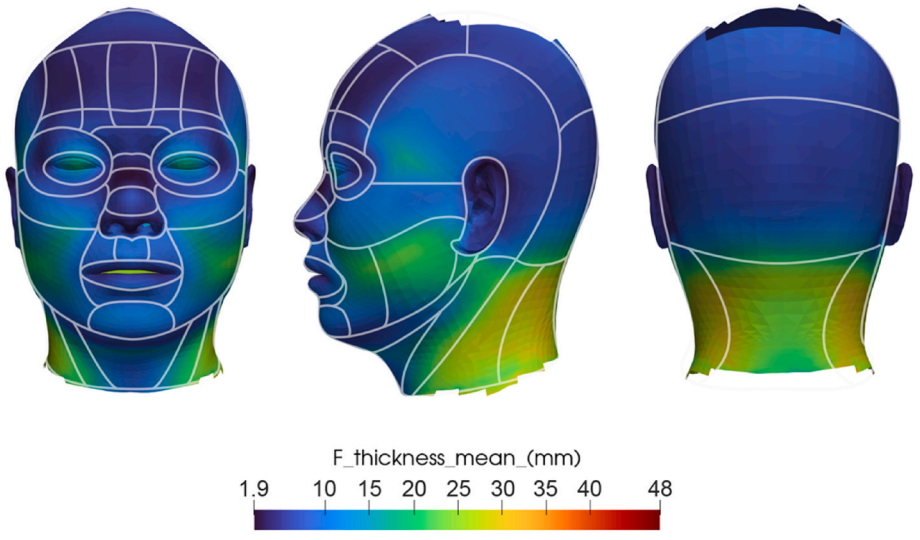


**Fig. 8.** Soft tissue thickness map (female).

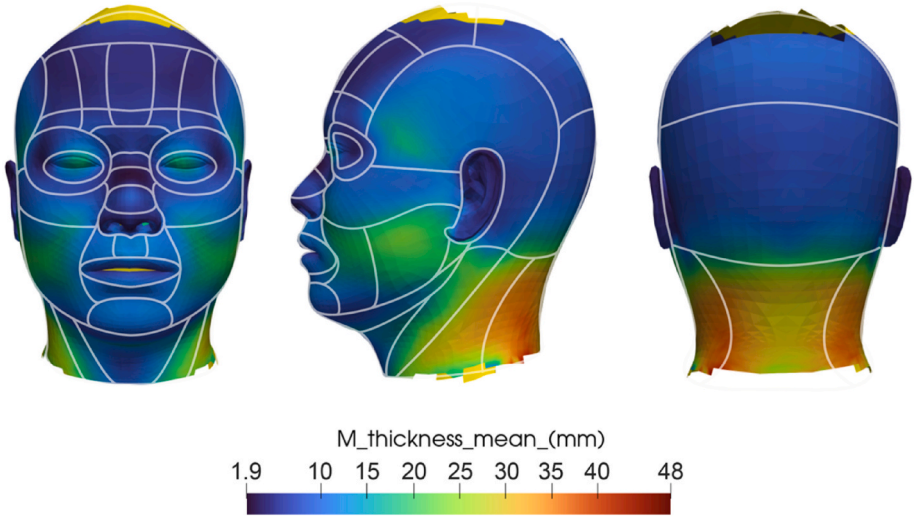


**Fig. 9.** Soft tissue thickness map (male).

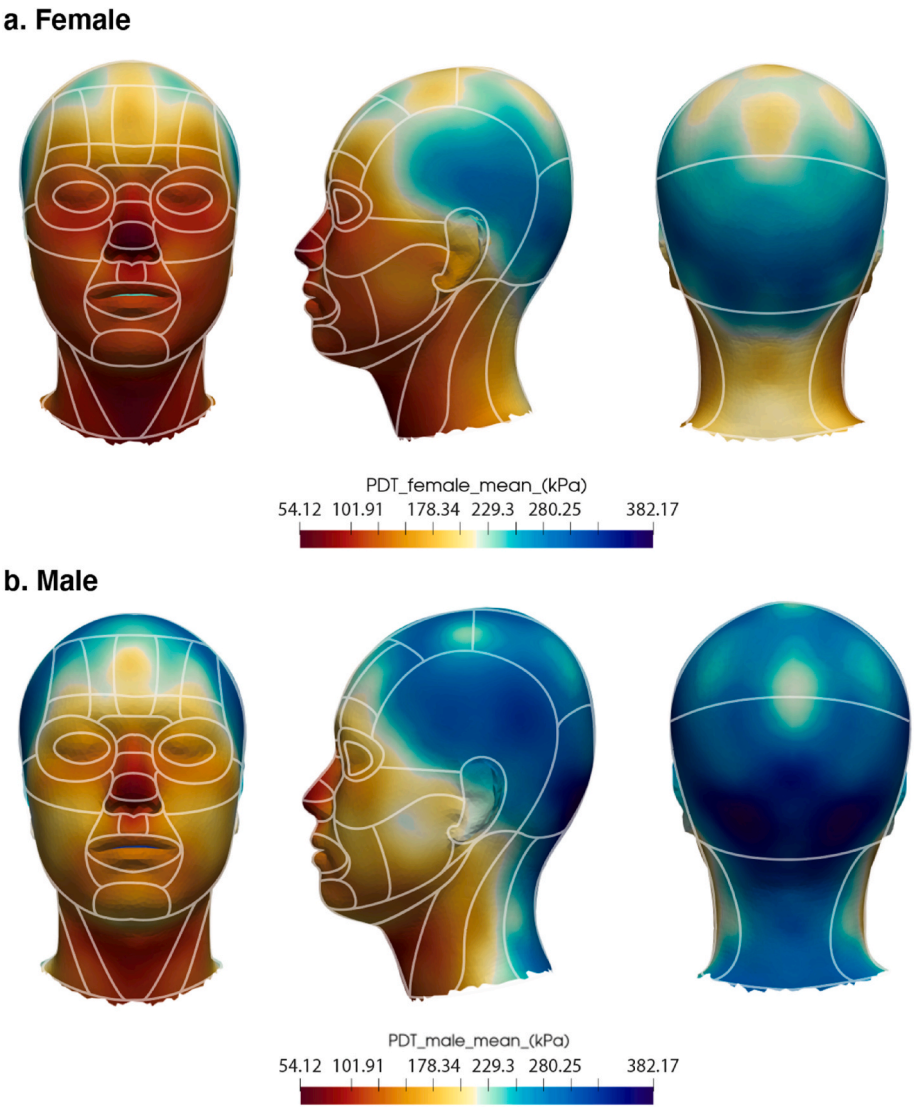


**Fig. 10.** PDT map a. Female b. Male.

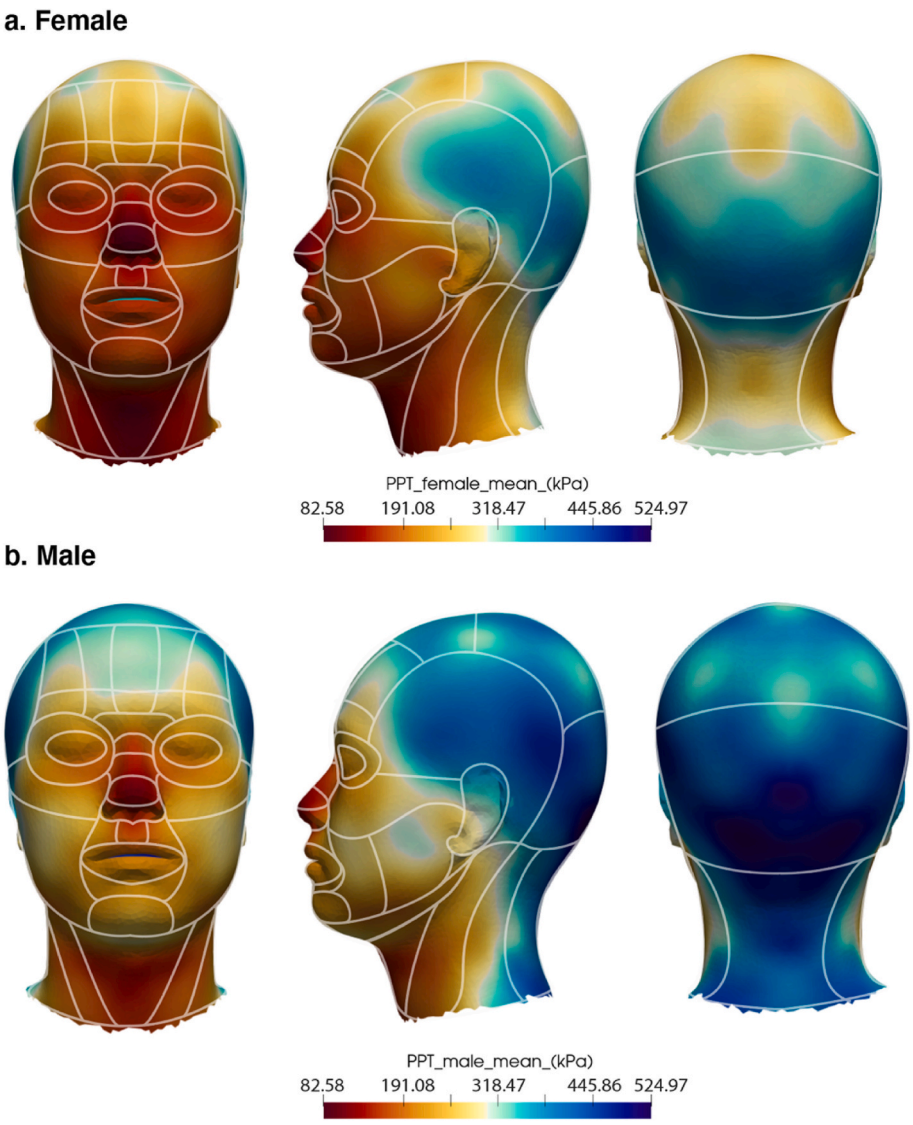


**Fig. 11.** PPT map a. Female b. Male.

under continuous pressure are summarized in Table 1(see appendix). The participants' PDT map (Fig. 6) and PPT map (Fig. 7) revealed similar trends for the head, face, and neck. The pressure value thresholds for the head were the highest, thus its sensitivity was the lowest, followed by the neck, and the face had the highest pressure sensitivity.

In the comparison of the gender groups, the PDT of 34.45% (41) landmarks showed a statistically significant difference ($p < 0.05$), and the mean PDT of all 41 landmarks in males was greater than that in females (appendix Table 2). At the same time, among the PPT of the 119 landmarks, 57.14% (68) showed a statistically significant difference ($p < 0.05$), and the mean PDT of all 68 landmarks in males was greater than that in females (appendix Table 3). In addition, in the comparison of the head, face, and neck, the PDT map (Fig. 10) and PPT map (Fig. 11) of men and women also showed similar trends. The pressure value thresholds for the head are the highest, while its sensitivity was the lowest, followed by the neck, and the face had the highest pressure sensitivity.

In addition to difference analysis between genders, this study also conducted a Pearson correlation coefficient analysis between PDT, PPT, and BMI to check for a link between obesity and sensitivity (Vink and Lips, 2017). The results showed that for female subjects, 66.38% (79) of the landmarks have a (positive) very weak correlation (0.0–0.2) or a weak correlation (0.2–0.4) between PDT and BMI, and 33.61% (40) of the landmarks were negatively correlated with BMI. In addition, 33.61% (40) of the landmarks showed a negative correlation between PPT and BMI, and the rest of the landmarks showed a statistically weak correlation (0.2–0.4). For male subjects, 36.13% (43) of the landmarks showed a statistically moderate correlation (0.4–0.6) between PDT and BMI and three landmarks show a strong correlation (0.6–1.0). In addition, similar to the trend for PDT, 36.13% (43) of the landmarks of PPT showed a statistically moderate correlation (0.4–0.6), and four landmarks showed a strong correlation (0.6–1.0). At the same time, PPT for three landmarks was negatively correlated with BMI.

In the comparison group of pressure threshold and soft tissue thickness, the pressure threshold (PDT and PPT) of all 28 landmarks showed a statistically weak correlation with soft tissue thickness. The Pearson correlation coefficient between female PDT and female soft tissue thickness was $-0.24$ ($p > 0.05$), and the correlation between PPT and soft tissue thickness was 0 ($p > 0.05$). In addition, the Pearson correlation coefficient between male PDT and male soft tissue thickness was $-0.02$ ($p > 0.05$), and the Pearson correlation coefficient between PPT and soft tissue thickness was 0 ($p > 0.05$) (Table 4). Figs. 8 and 9 demonstrate the division of 28 soft tissue thickness regions for men and women, and Figs. 10 and 11 show the division results of pressure sensitivity maps for men and women.

In addition to correlation analysis of pressure sensitivity thresholds

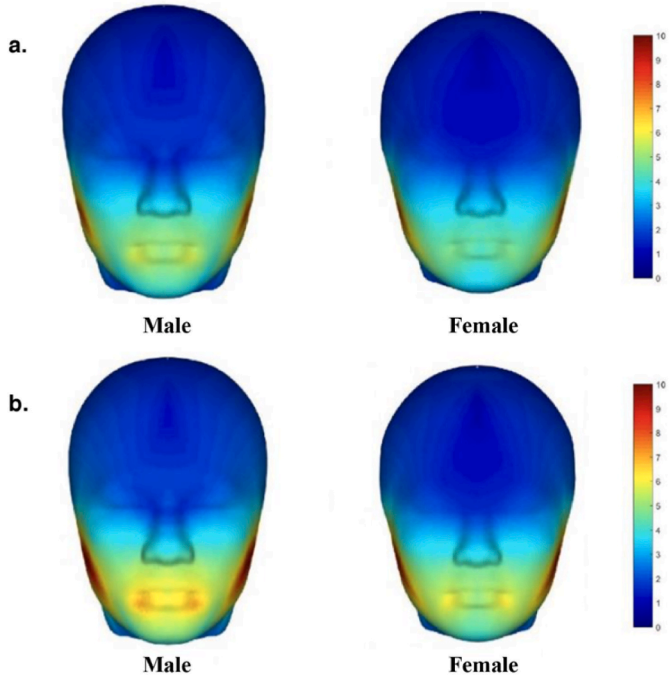


**Fig. 12.** Average tissue deformation map (unit:mm) a. Discomfort b. Pain (Shah et al., 2022).

**Table 5**
Data on pressure sensitivity, soft tissue thickness and soft tissue deformation of female.

| No. | Pressure sensitivity (kPa) | | Soft tissue thickness (mm) | Soft tissue deformation (mm) | |
|---|---|---|---|---|---|
| | PDT mean | PPT mean | Mean | PDT mean | PPT mean |
| 1 | 184.08 | 238.54 | 0 | 1.42 | 1.64 |
| 2 | 243.44 | 334.01 | 6.95 | 1.38 | 1.55 |
| 3 | 250.32 | 347.64 | 7.8 | 1.64 | 1.83 |
| 4 | 270.13 | 364.01 | 6.38 | 2.22 | 2.4 |
| 5 | 190.38 | 244.9 | 4.3 | 1.6 | 1.78 |
| 6 | 191.46 | 258.41 | 4.04 | 0.75 | 0.84 |
| 7 | 159.17 | 242.48 | 7.01 | 2.4 | 2.69 |
| 8 | 250.32 | 347.64 | 10.98 | 2 | 2.51 |
| 9 | 115.29 | 161.34 | 21.99 | 8.12 | 9.42 |
| 10 | 116.75 | 154.9 | 11.22 | 3.12 | 3.54 |
| 11 | 104.39 | 151.4 | 7.89 | 4.66 | 5.18 |
| 12 | 176.37 | 245.67 | 5.26 | 1.23 | 1.36 |
| 13 | 115.61 | 161.72 | 9.67 | 4.79 | 6.12 |
| 14 | 154.39 | 203.38 | 5.93 | 1.07 | 1.18 |
| 15 | 104.71 | 146.82 | 5.12 | 1.34 | 1.48 |
| 16 | 107.39 | 143.25 | 3.69 | 1.46 | 1.65 |
| 17 | 87.77 | 128.85 | 9.61 | 4.36 | 4.89 |
| 18 | 116.11 | 159.75 | 8.98 | 4.22 | 4.87 |

and soft tissue thickness data, this study also performed a correlation analysis among pressure sensitivity, soft tissue thickness, and the degree of soft tissue deformation under pressure discomfort and pressure pain conditions. Since the soft tissue deformation data used in this paper comes from Shah's paper (Kosek et al., 1993), the author selected 18 landmarks (unilateral) on the head and face, and tissue deformation at discomfort and pain threshold was measured (Fig. 12). Moreover, the pressure sensitivity map and soft tissue thickness data generated in this study include these 18 landmarks, so the correlation analysis among the three elements was performed based on the 18 landmarks.

The results showed that for female, the correlation coefficient between PDT and soft tissue thickness was −0.13 ($p > 0.05$), and the correlation coefficient between PPT and soft tissue thickness was −0.09 ($p > 0.05$). In addition, the correlation coefficient between PDT and PDT soft tissue deformation degree was −0.51($p < 0.05$), and the correlation coefficient between PPT and PPT soft tissue deformation degree was −0.47 (($p < 0.05$). The correlation coefficient between the degree of soft tissue deformation and soft tissue thickness in PDT was 0.75 ($p < 0.01$), and the correlation coefficient between soft tissue deformation and soft tissue thickness in PPT was 0.76 ($p < 0.01$) (Table 5). For male, the correlation coefficient between PDT and soft tissue thickness was −0.03 ($p > 0.05$), and the correlation coefficient between PPT and soft tissue thickness was 0 ($p > 0.05$). The correlation coefficient between PDT and PDT soft tissue deformation was −0.46 ($p > 0.05$), and the correlation coefficient between PPT and PPT soft tissue deformation was −0.39 (p-value $p > 0.05$). The correlation coefficient between PDT soft tissue deformation and soft tissue thickness was 0.75 ($p < 0.01$), and the correlation coefficient between PPT soft tissue deformation and soft tissue thickness was 0.77 ($p < 0.01$) (Table 6).

**Table 6**
Data on pressure sensitivity, soft tissue thickness and soft tissue deformation of male.

| No. | Pressure sensitivity (kPa) | | Soft tissue thickness (mm) | Soft tissue deformation (mm) | |
|---|---|---|---|---|---|
| | PDT mean | PPT mean | Mean | PDT mean | PPT mean |
| 1 | 233.6 | 331.61 | 0 | 1.35 | 1.59 |
| 2 | 293.87 | 396.26 | 8.76 | 1.7 | 1.92 |
| 3 | 309.71 | 429.54 | 8.92 | 2.03 | 2.23 |
| 4 | 323.49 | 471.18 | 7.07 | 2.18 | 2.45 |
| 5 | 235.67 | 323.81 | 4.98 | 1.44 | 1.63 |
| 6 | 257.88 | 359.55 | 4.53 | 0.97 | 1.1 |
| 7 | 219.35 | 328.5 | 7.43 | 2.51 | 2.73 |
| 8 | 309.71 | 429.54 | 13.19 | 2.26 | 2.81 |
| 9 | 167.91 | 266.48 | 22.76 | 8.26 | 10.14 |
| 10 | 146.02 | 223.89 | 10.54 | 3.15 | 3.87 |
| 11 | 141.64 | 219.11 | 7.73 | 3.83 | 4.64 |
| 12 | 213.69 | 306.21 | 5.51 | 1.75 | 1.96 |
| 13 | 140.45 | 215.29 | 11.27 | 5.77 | 7.02 |
| 14 | 186.91 | 269.82 | 6.17 | 1.61 | 1.79 |
| 15 | 120.38 | 163.61 | 5.94 | 1.92 | 2.16 |
| 16 | 128.58 | 180.89 | 3.83 | 1.37 | 1.52 |
| 17 | 106.45 | 154.7 | 11.28 | 4.76 | 5.56 |
| 18 | 143.79 | 216.8 | 9.93 | 4.96 | 5.79 |

## 4. Discussion and conclusion

The aim of this paper is to develop ways to reduce the pressure discomfort of head-related products by studying the relation between pressure sensitivity and soft tissue in the head, face and neck. Overall, the innovations of this study are mainly divided into the following:

Firstly, based on the PDT and PPT data for 36 subjects and 119 landmarks for each subject, this study generated high-precision pressure discomfort and pressure pain maps of the Chinese population's head, face, and neck. The results showed that the subjects' PDT map and PPT map have similar trends for the head, face, and neck. The head and back of the neck, which are connected to the occiput, have a distinct demarcation line from the other areas, and the PPT image was more prominent. Comparing the studied areas, the pressure value thresholds for the head were the highest, while its sensitivity was the lowest. Although the skull structure is relatively simple and the thickness of the soft tissue overlying the skull is relatively uniform (He et al., 2021), the pressure sensitivity of the head region is not uniform. The pressure sensitivity of the forehead has an interesting "M" shape. In particular, the PPT images of women showed radially sensitive areas of the parietal bone. There were also several ovals sensitive areas in the parietal and occipital bones, and the highest PDT and PPT value were experienced at the lower occipital bone, followed by the neck. Notably, the pressure sensitivity (PDT and PPT) of the back of the neck where it meets the occipital bone is significantly lower than in the anterior region. The

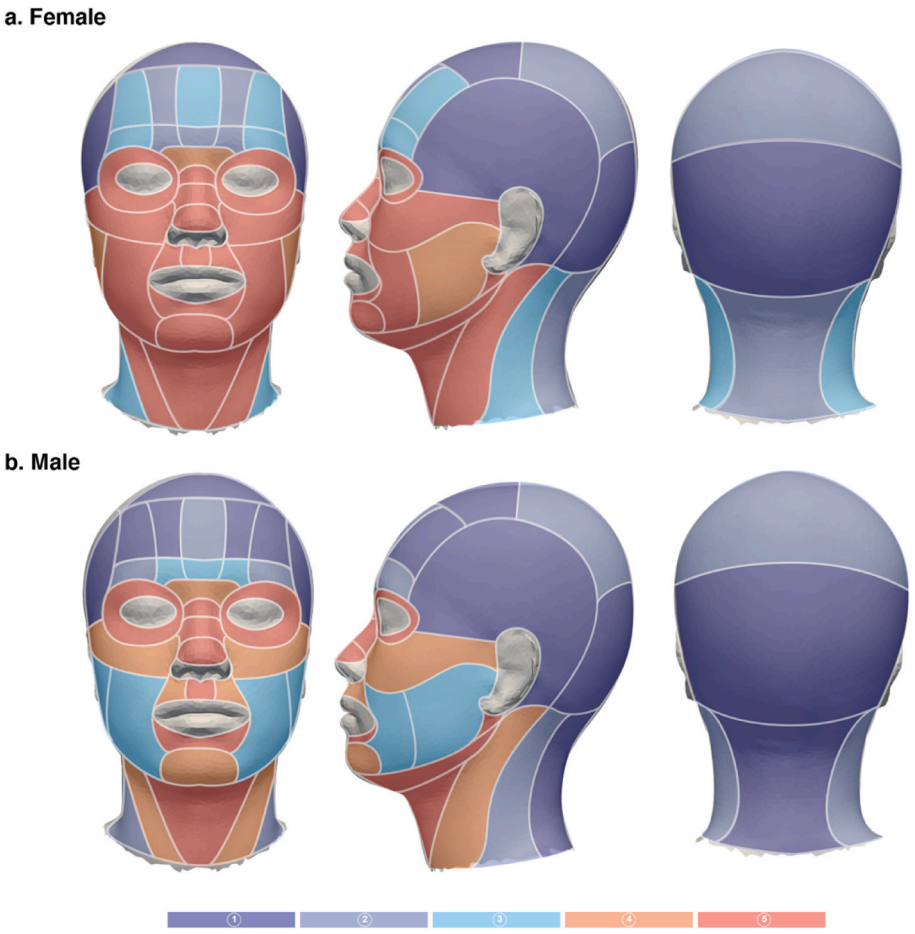


**Fig. 13.** Recommended map of the optimal pressure-bearing area.

sensitivity of the throat is also particularly high, second only to the tip of the nose. Finally, the face is the most sensitive to pressure, and its most sensitive area is the nose, particularly the tip of the nose. However, many head-related products, such as glasses, use the nose as the primary load-bearing area. Designers can consider reducing the pressure discomfort of head-related products in the future by changing the structure or material of the product to take advantage of this information. Also, the mid-nasolabial, lower orbital, and upper cheekbones are not ideal weight-bearing areas for the head-related product.

Compared with the results of other studies, Shah's (Shah and Luximon, 2021) Chinese head and face pressure discomfort and pressure pain map revealed that the upper part of the parietal bone was the least sensitive area in both men and women. However, according to the findings of this study, the lower part of the parietal bone and the occipital bone are the least sensitive areas. Furthermore, Shah's findings revealed that the face and nose are sensitive areas, which this paper's finding concurred with generally. In this study, however, the nose, particularly the tip of the nose, was found to be more sensitive than other facial areas. One explanation for the divergence in conclusions is the differing density of landmarks in both studies. In Europe, Broekhuizen (Broekhuizen et al., 2018)found that the upper part of the parietal bone and the occipital bone are very insensitive areas for both men and women, while the forehead is more sensitive, which this paper's finding concurred with generally. This suggests similarities in head pressure sensitivity between Europeans and Chinese.

In the comparison of the gender groups, women are more sensitive than men. This conclusion is consistent with other studies on pressure discomfort threshold and pressure pain threshold measurement (Vink and Lips, 2017; Binderup et al., 2010; Fredriksson et al., 2000). Gender differences should be considered in product design so that products can meet the needs of different groups of people. In addition to difference analysis between genders, this study also conducted a Pearson correlation coefficient analysis between PDT, PPT, and BMI. The results revealed no significant correlation between BMI and pressure discomfort or pressure pain.

Secondly, based on the high-precision Chinese soft tissue thickness map, anatomical structure map, and pressure sensitivity map, the head, face, and neck were divided into 28 regions (unilateral), and 28 anatomically corresponding landmarks were chosen for data extraction and analysis. The results showed that soft tissue thickness was not an essential factor affecting pressure sensitivity. Pressure sensitivity may be affected by other factors. The activation of tactile nerves, especially mechanoreceptors, is humans' primary cause of pressure perception (Johansson and Westling, 1984). This paper discusses the results of this study in terms of tactile innervation density and cortical topography, also known as the "sensory homunculus." The first is tactile innervation density. According to a study by Corniani et al. (Corniani and Saal, 2020), the hands and face are the most densely innervated regions across the whole body, especially the palmar skin of the hands and the perioral region of the face. In addition, the study noted that the innervation density was not uniform across the face, with 48 units/cm2 in the forehead, eyes, and nose, 67 units/cm2 in the central part of the face, and 84 units/cm2 in the lower lip, chin, and areas surrounding the ears. Moreover, concerning cortical topography in the cerebral cortex, previous studies have demonstrated that the face, particularly the perioral region, has a high proportion of cortical representations in the sensory cortex compared with the rest of the body (Kaas et al., 1979; Marshall et al., 1937). The conclusions of the above studies (high innervation

density and high cortical representation ratio) have a relatively consistent correspondence with the findings of this study (high pressure-sensitive areas). However, this does not mean that soft tissue thickness data is of no value in studies of pressure discomfort. For example, in the simulation experiments of testing head-related products, such as finite element stress experiments (Yang et al., 2022; Lei et al., 2012), the soft tissue thickness data of the human body is an essential basis for establishing an accurate finite element model.

Thirdly, in addition to correlation analysis of pressure sensitivity thresholds and soft tissue thickness data, this study also performed a correlation analysis on pressure sensitivity, soft tissue thickness, and the degree of soft tissue deformation under pressure discomfort and pressure pain conditions. The correlation analysis results in this section demonstrated that soft tissue thickness also tissue deformation were not essential factors influencing pressure sensitivity, but there is a statistically significant correlation between soft tissue thickness and the degree of soft tissue deformation ($p < 0.01$). The thicker the soft tissue, the greater the degree of soft tissue deformation, which is not unexpected. Furthermore, pressure thresholds (PDT and PPT) were moderately negatively correlated with soft tissue deformation in females($p < 0.05$). However, male pressure thresholds (PDT and PPT) and soft tissue deformation did not show significant differences, which could be attributed to the small sample size or data from different groups of subjects. Moreover, the discomfort is a subjective feeling (Vink and Hallbeck, 2012) , so subjective pressure discomfort and pain threshold are essential in studies of pressure discomfort.

Fourth, based on the above conclusions, a "recommended map" (Fig. 13) of the optimal stress-bearing area of the head, face and neck based on pressure sensitivity maps for head-related products was generated. In this figure, pressure sensitivity increases gradually from the purple area to the red area. Purple areas (1) are the most optimal weight-bearing part, followed by the dark blue areas (2), light blue areas (3) are more sensitive than the first two areas, while the orange areas (4) are more sensitive than the first three areas. The rest of red parts (5) are very sensitive areas and should not be used as the primary weight-bearing areas for head-related products.

However, this study also has limitations. First, this study's pressure discomfort/pain thresholds, soft tissue thickness data, and soft tissue PDT and PPT deformation data are not from the same set of samples, so this may influence the correlation analysis. Secondly, this study only collected data from one age group (18–30 years old). The next stage could be comparative research between different age groups and even different ethnic groups. Third, only one pressure gauge size was used in this paper and pressure sensitivity thresholds may be affected by various sizes and shapes of pressure probes. Finally, because most head-related products will cover multiple areas at once, the PDT and PPT values produced by applying pressure to multiple areas at once may differ from the PDT and PPT values produced by applying pressure to a single area. Research on these deficiencies can also help increase understanding of human body pressure discomfort.

The pressure sensitivity of the head, face, and neck are not the same, and there are gender differences in pressure sensitivity. Pressure sensation is caused by soft tissue deformation. However, according to the findings of this study, pressure sensitivity is not related to soft tissue thickness but may be related to the degree of soft tissue deformation. This demonstrates that studying pressure sensitivity solely from the standpoint of macroscopic morphology is insufficient and that other aspects, such as the distribution of mechanoreceptors, can be studied in the future. This type of research can help reduce pressure discomfort in wearable products.

## Declaration of competing interest

The authors declare that they have no known competing financial interests or personal relationships that could have appeared to influence the work reported in this paper.

## Acknowledgements

The authors would like to acknowledge the support of School of design Hunan University and the Faculty of Industrial Design Engineering, Delft University of Technology.

## Appendix

**Table 1**
PDT and PPT value for 36 participants (Unit: kPa)

| Landmark No. | PDT Mean | PDT SD | PPT Mean | PPT SD | Landmark No. | PDT Mean | PDT SD | PPT Mean | PPT SD |
|---|---|---|---|---|---|---|---|---|---|
| 1 | 177.60 | 57.55 | 270.74 | 85.24 | 40 | 198.41 | 82.26 | 257.78 | 103.56 |
| 2 | 168.40 | 49.40 | 232.91 | 78.08 | 41 | 252.83 | 118.28 | 334.08 | 132.22 |
| 3 | 111.68 | 34.09 | 154.28 | 50.18 | 42 | 185.92 | 80.83 | 280.71 | 105.61 |
| 4 | 92.22 | 40.84 | 127.85 | 50.62 | 43 | 248.76 | 115.22 | 358.07 | 149.96 |
| 5 | 60.05 | 23.79 | 92.71 | 31.88 | 44 | 206.09 | 83.36 | 279.90 | 126.84 |
| 6 | 96.07 | 36.76 | 140.34 | 53.32 | 45 | 210.51 | 82.22 | 279.97 | 113.66 |
| 7 | 128.41 | 45.52 | 185.10 | 60.62 | 46 | 248.12 | 103.81 | 329.16 | 131.00 |
| 8 | 133.65 | 54.59 | 204.10 | 86.07 | 47 | 276.72 | 129.11 | 384.04 | 144.66 |
| 9 | 116.81 | 46.21 | 159.98 | 59.71 | 48 | 283.86 | 126.05 | 383.23 | 141.92 |
| 10 | 113.52 | 57.45 | 155.20 | 69.64 | 49 | 251.45 | 113.71 | 323.64 | 123.92 |
| 11 | 145.86 | 55.68 | 205.98 | 74.54 | 50 | 210.05 | 89.77 | 280.71 | 107.40 |
| 12 | 151.98 | 79.41 | 214.44 | 93.19 | 51 | 273.07 | 126.22 | 359.62 | 133.90 |
| 13 | 122.68 | 64.46 | 185.24 | 81.21 | 52 | 242.89 | 104.99 | 318.15 | 133.82 |
| 14 | 126.65 | 57.84 | 185.53 | 74.11 | 53 | 252.97 | 129.82 | 342.43 | 157.83 |
| 15 | 120.95 | 43.44 | 181.49 | 76.31 | 54 | 265.85 | 132.66 | 361.68 | 157.34 |
| 16 | 125.62 | 65.72 | 192.50 | 86.11 | 55 | 220.98 | 81.92 | 303.36 | 127.48 |
| 17 | 120.74 | 64.69 | 178.13 | 80.87 | 56 | 259.70 | 123.81 | 348.37 | 153.28 |
| 18 | 129.76 | 46.64 | 185.56 | 75.08 | 57 | 253.40 | 118.28 | 331.60 | 127.96 |
| 19 | 148.34 | 80.07 | 233.33 | 106.10 | 58 | 220.63 | 85.29 | 316.31 | 132.49 |
| 20 | 175.97 | 89.49 | 253.01 | 108.98 | 59 | 255.63 | 129.85 | 339.07 | 157.38 |
| 21 | 178.77 | 83.23 | 263.38 | 113.47 | 60 | 210.05 | 83.78 | 289.70 | 114.32 |
| 22 | 138.68 | 62.92 | 208.07 | 88.25 | 61 | 225.51 | 99.77 | 317.20 | 144.06 |
| 23 | 137.97 | 74.82 | 205.73 | 103.73 | 62 | 318.08 | 154.26 | 445.61 | 185.68 |
| 24 | 139.21 | 63.71 | 197.06 | 74.37 | 63 | 293.84 | 136.31 | 411.64 | 189.81 |
| 25 | 115.89 | 52.65 | 161.75 | 74.38 | 64 | 277.88 | 134.85 | 392.18 | 173.70 |
| 26 | 120.10 | 65.06 | 166.45 | 84.42 | 65 | 238.85 | 102.22 | 321.94 | 131.00 |

(*continued on next page*)

**Table 1** (*continued*)

| Landmark No. | PDT Mean | PDT SD | PPT Mean | PPT SD | Landmark No. | PDT Mean | PDT SD | PPT Mean | PPT SD |
|---|---|---|---|---|---|---|---|---|---|
| 27 | 139.56 | 65.03 | 195.79 | 78.75 | 66 | 274.88 | 143.69 | 367.52 | 166.23 |
| 28 | 128.27 | 67.14 | 176.89 | 82.25 | 67 | 303.40 | 131.68 | 402.94 | 159.46 |
| 29 | 113.87 | 61.76 | 176.19 | 83.90 | 68 | 288.50 | 141.00 | 403.47 | 159.79 |
| 30 | 130.93 | 77.77 | 199.75 | 109.20 | 69 | 267.09 | 133.34 | 363.31 | 174.15 |
| 31 | 138.68 | 72.60 | 210.44 | 110.17 | 70 | 231.74 | 116.87 | 331.63 | 156.73 |
| 32 | 156.69 | 95.12 | 229.30 | 124.00 | 71 | 262.53 | 147.65 | 352.34 | 178.50 |
| 33 | 180.47 | 90.17 | 244.73 | 109.10 | 72 | 259.98 | 112.66 | 337.93 | 142.25 |
| 34 | 171.97 | 75.74 | 239.00 | 91.66 | 73 | 220.77 | 89.18 | 291.51 | 122.07 |
| 35 | 167.66 | 68.05 | 240.23 | 98.51 | 74 | 271.27 | 126.22 | 376.68 | 158.83 |
| 36 | 160.23 | 69.29 | 212.35 | 84.97 | 75 | 297.03 | 122.17 | 401.13 | 150.85 |
| 37 | 175.34 | 76.20 | 235.07 | 102.33 | 76 | 328.73 | 182.83 | 433.47 | 200.91 |
| 38 | 192.96 | 88.99 | 272.58 | 110.79 | 77 | 256.40 | 127.37 | 358.35 | 170.71 |
| 39 | 232.24 | 98.51 | 311.00 | 133.65 | 78 | 268.05 | 119.59 | 366.07 | 155.71 |
| 79 | 289.10 | 122.94 | 394.41 | 159.68 | 100 | 207.57 | 116.63 | 289.38 | 138.31 |
| 80 | 268.90 | 126.43 | 359.34 | 162.18 | 101 | 185.63 | 95.02 | 267.59 | 124.09 |
| 81 | 326.40 | 127.69 | 445.79 | 174.29 | 102 | 223.14 | 124.63 | 340.06 | 165.38 |
| 82 | 315.29 | 158.45 | 431.63 | 184.39 | 103 | 170.67 | 78.08 | 246.14 | 113.18 |
| 83 | 241.76 | 142.05 | 341.22 | 184.10 | 104 | 133.51 | 78.88 | 191.65 | 104.01 |
| 84 | 228.80 | 121.88 | 336.91 | 173.52 | 105 | 109.13 | 65.19 | 160.79 | 87.00 |
| 85 | 246.32 | 132.74 | 363.69 | 181.25 | 106 | 102.34 | 52.69 | 150.67 | 80.46 |
| 86 | 247.45 | 159.65 | 332.94 | 185.61 | 107 | 97.24 | 44.46 | 145.58 | 64.64 |
| 87 | 227.88 | 122.54 | 328.91 | 174.81 | 108 | 103.68 | 49.70 | 152.41 | 69.40 |
| 88 | 253.04 | 139.43 | 367.02 | 194.51 | 109 | 85.67 | 53.11 | 131.88 | 84.07 |
| 89 | 241.83 | 121.27 | 348.30 | 168.64 | 110 | 91.79 | 52.53 | 138.64 | 63.37 |
| 90 | 176.96 | 94.50 | 270.52 | 130.28 | 111 | 80.25 | 40.50 | 120.03 | 68.10 |
| 91 | 160.16 | 82.35 | 234.39 | 106.13 | 112 | 81.74 | 49.08 | 120.24 | 67.63 |
| 92 | 147.59 | 79.11 | 213.94 | 106.89 | 113 | 135.46 | 66.63 | 203.86 | 97.37 |
| 93 | 125.80 | 69.26 | 174.52 | 88.60 | 114 | 75.87 | 42.01 | 112.49 | 57.43 |
| 94 | 122.47 | 61.69 | 181.99 | 89.61 | 115 | 69.57 | 31.98 | 103.89 | 52.85 |
| 95 | 177.67 | 107.10 | 253.29 | 118.80 | 116 | 321.80 | 146.99 | 461.50 | 179.15 |
| 96 | 113.48 | 58.32 | 172.05 | 87.56 | 117 | 335.60 | 169.65 | 434.93 | 194.76 |
| 97 | 142.64 | 68.45 | 204.95 | 95.15 | 118 | 262.95 | 101.80 | 350.00 | 144.29 |
| 98 | 157.71 | 81.23 | 236.98 | 107.76 | 119 | 283.16 | 161.13 | 378.52 | 185.34 |
| 99 | 181.35 | 98.04 | 258.74 | 122.83 | | | | | |

NS: no significant. *$p < 0.05$, **$p < 0.01$.

**Table 2**
PDT for gender difference (Unit: kPa)

| Landmark No. | Female | | | Male | | | Gender diff. |
|---|---|---|---|---|---|---|---|
| | Mean | SD | Correlation with BMI | Mean | SD | Correlation with BMI | |
| 1 | 173.31 | 60.51 | 0.02 | 182.96 | 55.09 | 0.24 | NS |
| 2 | 154.39 | 43.31 | 0.32 | 185.91 | 52.25 | 0.21 | P < 0.05 |
| 3 | 104.71 | 27.66 | 0.26 | 120.38 | 39.95 | 0.11 | NS |
| 4 | 84.65 | 35.72 | 0.26 | 101.67 | 45.86 | 0.11 | NS |
| 5 | 54.01 | 20.07 | −0.22 | 67.60 | 26.47 | 0.00 | NS |
| 6 | 87.77 | 37.14 | −0.22 | 106.45 | 34.62 | 0.21 | NS |
| 7 | 116.11 | 46.00 | −0.07 | 143.79 | 41.24 | 0.35 | NS |
| 8 | 116.50 | 52.07 | −0.05 | 155.10 | 51.34 | 0.33 | P < 0.05 |
| 9 | 107.39 | 40.76 | −0.36 | 128.58 | 51.11 | 0.11 | NS |
| 10 | 99.43 | 59.44 | −0.13 | 131.13 | 51.28 | 0.24 | NS |
| 11 | 130.13 | 46.43 | 0.10 | 165.53 | 61.33 | 0.34 | P < 0.05 |
| 12 | 131.72 | 79.07 | −0.02 | 177.31 | 74.60 | 0.31 | NS |
| 13 | 98.66 | 57.85 | −0.01 | 152.71 | 61.03 | 0.39 | P < 0.01 |
| 14 | 115.61 | 65.95 | 0.00 | 140.45 | 43.93 | 0.30 | NS |
| 15 | 104.39 | 38.56 | −0.10 | 141.64 | 41.20 | 0.36 | P < 0.01 |
| 16 | 117.39 | 64.12 | −0.09 | 135.91 | 68.31 | 0.37 | NS |
| 17 | 100.00 | 61.48 | −0.23 | 146.66 | 60.73 | 0.34 | P < 0.05 |
| 18 | 116.75 | 50.53 | 0.16 | 146.02 | 36.52 | 0.21 | NS |
| 19 | 116.94 | 58.32 | −0.14 | 187.58 | 87.72 | 0.46 | P < 0.01 |
| 20 | 145.92 | 72.94 | 0.02 | 213.54 | 96.12 | 0.43 | P < 0.05 |
| 21 | 150.83 | 63.90 | 0.14 | 213.69 | 93.01 | 0.35 | P < 0.05 |
| 22 | 115.29 | 57.62 | 0.00 | 167.91 | 58.23 | 0.14 | P < 0.05 |
| 23 | 110.70 | 58.73 | 0.10 | 172.05 | 80.39 | 0.15 | P < 0.01 |
| 24 | 114.78 | 43.48 | 0.00 | 169.75 | 72.70 | 0.34 | P < 0.01 |
| 25 | 102.55 | 44.68 | 0.02 | 132.56 | 58.35 | 0.39 | NS |
| 26 | 110.45 | 68.20 | 0.01 | 132.17 | 60.87 | 0.48 | NS |
| 27 | 121.78 | 56.88 | 0.10 | 161.78 | 69.45 | 0.47 | NS |
| 28 | 113.25 | 55.98 | 0.11 | 147.05 | 76.64 | 0.40 | NS |
| 29 | 101.66 | 56.57 | −0.14 | 129.14 | 66.33 | 0.23 | NS |
| 30 | 109.30 | 64.62 | −0.04 | 157.96 | 86.14 | 0.31 | NS |
| 31 | 118.41 | 68.06 | 0.02 | 164.01 | 72.10 | 0.39 | P < 0.05 |
| 32 | 129.68 | 59.79 | −0.05 | 190.45 | 119.98 | 0.42 | P < 0.05 |

(*continued on next page*)

**Table 2** (*continued*)

| Landmark No. | Female | | | Male | | | Gender diff. |
|---|---|---|---|---|---|---|---|
| | Mean | SD | Correlation with BMI | Mean | SD | Correlation with BMI | |
| 33 | 151.97 | 70.01 | −0.14 | 216.08 | 101.63 | 0.40 | $P < 0.05$ |
| 34 | 139.24 | 70.96 | 0.17 | 212.90 | 61.56 | 0.18 | $P < 0.01$ |
| 35 | 136.43 | 57.19 | 0.34 | 206.69 | 61.14 | 0.29 | $P < 0.01$ |
| 36 | 134.84 | 57.69 | 0.21 | 191.96 | 71.08 | 0.13 | $P < 0.01$ |
| 37 | 151.72 | 78.43 | 0.17 | 204.86 | 63.91 | 0.13 | $P < 0.05$ |
| 38 | 176.37 | 89.89 | 0.25 | 213.69 | 86.12 | 0.17 | NS |
| 39 | 218.28 | 110.50 | 0.14 | 249.68 | 81.17 | 0.40 | NS |
| 40 | 176.94 | 76.62 | 0.08 | 225.24 | 83.49 | 0.32 | NS |
| 41 | 217.71 | 109.30 | 0.10 | 296.74 | 117.52 | 0.26 | $P < 0.05$ |
| 42 | 159.17 | 81.49 | 0.07 | 219.35 | 68.47 | 0.50 | $P < 0.05$ |
| 43 | 230.64 | 136.26 | 0.09 | 271.42 | 80.45 | 0.20 | NS |
| 44 | 184.08 | 71.57 | 0.04 | 233.60 | 90.94 | −0.06 | NS |
| 45 | 190.38 | 87.81 | 0.11 | 235.67 | 69.21 | 0.22 | NS |
| 46 | 212.10 | 82.92 | −0.14 | 293.15 | 112.00 | 0.20 | $P < 0.01$ |
| 47 | 250.32 | 131.26 | 0.13 | 309.71 | 122.41 | 0.36 | NS |
| 48 | 265.03 | 129.40 | 0.08 | 307.40 | 121.66 | 0.40 | NS |
| 49 | 207.07 | 93.99 | −0.02 | 306.93 | 114.33 | 0.28 | $P < 0.01$ |
| 50 | 187.52 | 94.54 | 0.12 | 238.22 | 77.18 | 0.15 | NS |
| 51 | 251.66 | 134.53 | 0.07 | 299.84 | 113.46 | 0.28 | NS |
| 52 | 205.35 | 84.20 | −0.01 | 289.81 | 111.86 | 0.24 | $P < 0.01$ |
| 53 | 228.85 | 151.89 | 0.12 | 283.12 | 91.42 | 0.45 | NS |
| 54 | 243.44 | 141.74 | 0.12 | 293.87 | 118.78 | 0.18 | NS |
| 55 | 191.46 | 70.64 | −0.06 | 257.88 | 82.00 | 0.05 | $P < 0.01$ |
| 56 | 244.20 | 144.63 | 0.16 | 279.06 | 92.47 | 0.34 | NS |
| 57 | 216.94 | 111.03 | 0.18 | 298.96 | 114.20 | 0.21 | $P < 0.05$ |
| 58 | 202.87 | 84.94 | 0.00 | 242.83 | 83.00 | 0.36 | NS |
| 59 | 224.78 | 114.50 | −0.15 | 294.19 | 140.99 | 0.18 | NS |
| 60 | 201.66 | 86.98 | −0.19 | 220.54 | 81.14 | 0.21 | NS |
| 61 | 203.44 | 92.39 | −0.11 | 253.11 | 104.65 | 0.35 | NS |
| 62 | 282.48 | 162.39 | 0.08 | 362.58 | 135.36 | 0.43 | NS |
| 63 | 270.13 | 135.19 | 0.06 | 323.49 | 136.09 | 0.40 | NS |
| 64 | 227.39 | 109.71 | 0.23 | 341.00 | 139.76 | 0.38 | $P < 0.01$ |
| 65 | 211.15 | 89.33 | −0.18 | 273.49 | 109.41 | 0.19 | NS |
| 66 | 257.64 | 169.16 | 0.14 | 296.42 | 105.06 | 0.19 | NS |
| 67 | 278.47 | 141.63 | 0.07 | 334.55 | 114.84 | 0.16 | NS |
| 68 | 282.68 | 157.12 | 0.07 | 295.78 | 122.55 | 0.15 | NS |
| 69 | 259.81 | 162.27 | 0.07 | 276.19 | 89.29 | 0.09 | NS |
| 70 | 221.08 | 132.80 | 0.02 | 245.06 | 95.89 | .51* | NS |
| 71 | 235.10 | 165.44 | 0.07 | 296.82 | 118.06 | 0.17 | NS |
| 72 | 227.39 | 108.23 | −0.08 | 300.72 | 107.67 | 0.25 | $P < 0.05$ |
| 73 | 204.27 | 93.93 | −0.03 | 241.40 | 81.03 | 0.35 | NS |
| 74 | 248.92 | 129.48 | 0.06 | 299.20 | 120.16 | 0.35 | NS |
| 75 | 276.82 | 138.34 | −0.10 | 322.29 | 96.74 | 0.21 | NS |
| 76 | 318.66 | 215.55 | 0.14 | 341.32 | 137.24 | 0.29 | NS |
| 77 | 229.43 | 132.86 | 0.22 | 290.13 | 115.39 | 0.16 | NS |
| 78 | 242.55 | 120.40 | 0.01 | 299.92 | 114.27 | 0.36 | NS |
| 79 | 270.76 | 125.43 | −0.01 | 312.02 | 119.71 | 0.32 | NS |
| 80 | 236.88 | 112.96 | 0.11 | 308.92 | 134.39 | 0.30 | NS |
| 81 | 292.80 | 120.65 | 0.04 | 368.39 | 127.35 | .50* | NS |
| 82 | 296.11 | 184.23 | 0.18 | 339.25 | 120.37 | 0.42 | NS |
| 83 | 193.06 | 121.45 | 0.21 | 302.63 | 145.89 | .58* | $P < 0.01$ |
| 84 | 194.84 | 110.41 | 0.03 | 271.26 | 125.54 | 0.45 | NS |
| 85 | 209.55 | 118.85 | 0.13 | 292.28 | 138.45 | 0.44 | NS |
| 86 | 210.51 | 175.98 | 0.23 | 293.63 | 127.08 | 0.25 | NS |
| 87 | 171.02 | 87.72 | −0.12 | 298.96 | 124.86 | 0.46 | $P < 0.05$ |
| 88 | 196.43 | 118.03 | 0.13 | 323.81 | 134.55 | 0.47 | $P < 0.01$ |
| 89 | 196.62 | 111.84 | 0.10 | 298.33 | 111.08 | 0.41 | $P < 0.01$ |
| 90 | 149.75 | 87.68 | 0.00 | 210.99 | 94.23 | 0.45 | $P < 0.01$ |
| 91 | 136.05 | 77.24 | 0.10 | 190.29 | 80.77 | 0.56* | $P < 0.05$ |
| 92 | 134.33 | 76.85 | 0.17 | 164.17 | 81.20 | 0.44 | NS |
| 93 | 110.51 | 69.73 | −0.02 | 144.90 | 65.82 | 0.44 | NS |
| 94 | 111.15 | 59.20 | 0.00 | 136.62 | 63.69 | .54* | NS |
| 95 | 139.94 | 97.66 | 0.03 | 224.84 | 102.04 | .50* | $P < 0.01$ |
| 96 | 93.69 | 48.15 | 0.16 | 138.22 | 61.85 | 0.25 | $P < 0.05$ |
| 97 | 135.86 | 68.28 | 0.15 | 151.11 | 69.94 | .51* | NS |
| 98 | 137.01 | 76.23 | 0.04 | 183.60 | 82.16 | .60* | NS |
| 99 | 157.45 | 78.11 | −0.04 | 211.23 | 113.95 | .64** | NS |
| 100 | 165.22 | 102.03 | 0.19 | 260.51 | 114.77 | 0.43 | $P < 0.01$ |
| 101 | 164.90 | 92.59 | 0.06 | 211.54 | 94.43 | 0.48 | NS |
| 102 | 182.29 | 102.53 | −0.06 | 274.20 | 133.86 | .64** | $P < 0.05$ |
| 103 | 141.66 | 62.93 | −0.16 | 206.93 | 81.75 | 0.43 | $P < 0.01$ |
| 104 | 115.48 | 66.26 | −0.10 | 156.05 | 89.33 | 0.44 | NS |
| 105 | 99.11 | 74.57 | 0.24 | 121.66 | 50.70 | 0.34 | NS |
| 106 | 90.19 | 55.17 | −0.03 | 117.52 | 46.70 | 0.47 | NS |

(*continued on next page*)

**Table 2** (*continued*)

| Landmark No. | Female | | | Male | | | Gender diff. |
|---|---|---|---|---|---|---|---|
| | Mean | SD | Correlation with BMI | Mean | SD | Correlation with BMI | |
| 107 | 97.07 | 43.43 | 0.00 | 97.45 | 47.15 | .52* | NS |
| 108 | 90.00 | 45.97 | 0.03 | 120.78 | 50.26 | .52* | NS |
| 109 | 81.59 | 54.43 | −0.06 | 90.76 | 52.71 | 0.31 | NS |
| 110 | 83.06 | 50.78 | 0.11 | 102.71 | 54.26 | 0.48 | NS |
| 111 | 77.90 | 43.32 | −0.21 | 83.20 | 37.86 | .55* | NS |
| 112 | 76.75 | 51.61 | −0.02 | 87.98 | 46.61 | .56* | NS |
| 113 | 108.41 | 58.56 | −0.14 | 169.27 | 61.81 | .51* | P < 0.01 |
| 114 | 67.07 | 34.10 | −0.01 | 86.86 | 49.13 | .54* | NS |
| 115 | 62.04 | 30.74 | 0.02 | 78.98 | 31.93 | 0.44 | NS |
| 116 | 313.44 | 169.13 | 0.19 | 332.25 | 118.19 | 0.37 | NS |
| 117 | 309.04 | 201.02 | 0.24 | 368.79 | 117.73 | 0.49 | NS |
| 118 | 227.01 | 93.69 | 0.03 | 307.88 | 95.83 | 0.26 | P < 0.01 |
| 119 | 286.94 | 171.56 | 0.03 | 278.42 | 152.49 | 0.07 | NS |

NS: no significant. *p < 0.05, **p < 0.01.

**Table 3**
PPT for gender difference (Unit: kPa)

| Landmark No. | Female | | | Male | | | Gender diff. |
|---|---|---|---|---|---|---|---|
| | Mean | SD | Correlation with BMI | Mean | SD | Correlation with BMI | |
| 1 | 242.80 | 75.36 | 0.07 | 305.65 | 86.12 | −0.06 | P < 0.05 |
| 2 | 203.38 | 64.49 | 0.28 | 269.82 | 79.63 | 0.07 | P < 0.01 |
| 3 | 146.82 | 44.01 | 0.22 | 163.61 | 57.05 | 0.03 | NS |
| 4 | 117.45 | 45.13 | −0.32 | 140.84 | 55.45 | 0.22 | NS |
| 5 | 82.55 | 28.79 | −0.20 | 105.41 | 31.80 | 0.05 | P < 0.05 |
| 6 | 128.85 | 54.45 | −0.09 | 154.70 | 49.82 | 0.37 | NS |
| 7 | 159.75 | 47.22 | −0.04 | 216.80 | 61.82 | 0.27 | P < 0.01 |
| 8 | 171.46 | 70.25 | −0.40 | 244.90 | 88.53 | 0.30 | P < 0.01 |
| 9 | 143.25 | 48.49 | −0.21 | 180.89 | 67.10 | 0.16 | P < 0.05 |
| 10 | 137.90 | 73.75 | 0.20 | 176.83 | 59.40 | 0.24 | NS |
| 11 | 176.50 | 58.70 | 0.15 | 242.83 | 77.41 | 0.26 | P < 0.01 |
| 12 | 187.83 | 102.13 | 0.05 | 247.69 | 70.19 | 0.40 | P < 0.05 |
| 13 | 155.41 | 67.84 | −0.02 | 222.53 | 83.00 | 0.32 | P < 0.01 |
| 14 | 161.72 | 79.57 | −0.13 | 215.29 | 55.63 | 0.44 | P < 0.05 |
| 15 | 151.40 | 63.99 | −0.17 | 219.11 | 75.39 | 0.47 | P < 0.01 |
| 16 | 169.11 | 86.31 | −0.23 | 221.74 | 78.89 | 0.47 | NS |
| 17 | 151.21 | 78.23 | 0.08 | 211.78 | 73.02 | 0.40 | P < 0.05 |
| 18 | 154.90 | 65.58 | 0.11 | 223.89 | 69.90 | 0.00 | P < 0.01 |
| 19 | 191.27 | 88.15 | −0.07 | 285.91 | 105.44 | 0.45 | P < 0.01 |
| 20 | 208.66 | 89.58 | 0.08 | 308.44 | 107.92 | 0.29 | P < 0.01 |
| 21 | 221.34 | 102.17 | 0.18 | 315.92 | 107.33 | 0.39 | P < 0.01 |
| 22 | 161.34 | 64.55 | 0.03 | 266.48 | 79.64 | 0.23 | P < 0.01 |
| 23 | 162.87 | 73.95 | 0.13 | 259.32 | 112.54 | 0.16 | P < 0.01 |
| 24 | 167.26 | 44.58 | 0.06 | 234.32 | 87.88 | 0.32 | P < 0.01 |
| 25 | 144.33 | 70.29 | 0.07 | 183.52 | 75.77 | 0.44 | NS |
| 26 | 152.36 | 82.01 | −0.06 | 184.08 | 86.69 | 0.41 | NS |
| 27 | 174.08 | 70.73 | 0.11 | 222.93 | 81.98 | 0.53* | NS |
| 28 | 152.61 | 64.12 | 0.18 | 207.25 | 93.86 | 0.38 | P < 0.05 |
| 29 | 156.82 | 76.19 | −0.18 | 200.40 | 89.14 | 0.39 | NS |
| 30 | 170.32 | 98.68 | −0.10 | 236.54 | 113.55 | 0.12 | NS |
| 31 | 173.82 | 83.63 | −0.07 | 256.21 | 124.25 | 0.27 | P < 0.05 |
| 32 | 183.95 | 80.98 | −0.07 | 285.99 | 146.29 | 0.41 | P < 0.05 |
| 33 | 209.62 | 79.22 | −0.26 | 288.61 | 126.98 | 0.33 | P < 0.05 |
| 34 | 201.27 | 76.83 | 0.06 | 286.15 | 88.63 | 0.08 | P < 0.01 |
| 35 | 194.84 | 83.95 | 0.21 | 296.97 | 86.79 | 0.12 | P < 0.01 |
| 36 | 173.95 | 65.75 | 0.17 | 260.35 | 83.33 | 0.10 | P < 0.01 |
| 37 | 199.87 | 93.29 | 0.17 | 279.06 | 98.46 | −0.01 | P < 0.01 |
| 38 | 245.67 | 111.92 | 0.12 | 306.21 | 102.97 | 0.17 | NS |
| 39 | 296.75 | 159.52 | 0.15 | 328.82 | 94.03 | 0.37 | NS |
| 40 | 224.97 | 84.19 | 0.07 | 298.81 | 113.21 | 0.16 | P < 0.05 |
| 41 | 296.88 | 136.64 | 0.14 | 380.57 | 113.98 | 0.36 | P < 0.05 |
| 42 | 242.48 | 107.16 | 0.24 | 328.50 | 84.23 | .54* | P < 0.05 |
| 43 | 316.88 | 149.05 | 0.12 | 409.55 | 138.71 | 0.18 | NS |
| 44 | 238.54 | 97.33 | 0.03 | 331.61 | 142.85 | −0.01 | P < 0.05 |
| 45 | 244.90 | 106.89 | 0.08 | 323.81 | 109.46 | 0.11 | P < 0.05 |
| 46 | 290.25 | 109.81 | −0.06 | 377.79 | 142.22 | 0.15 | P < 0.05 |
| 47 | 347.64 | 150.74 | 0.17 | 429.54 | 126.77 | 0.24 | NS |
| 48 | 358.60 | 144.11 | 0.11 | 414.01 | 137.38 | 0.43 | NS |
| 49 | 271.21 | 96.52 | 0.02 | 389.17 | 125.65 | 0.35 | P < 0.01 |
| 50 | 249.75 | 112.87 | 0.03 | 319.43 | 88.90 | 0.16 | P < 0.05 |
| 51 | 330.96 | 140.69 | −0.02 | 395.46 | 119.56 | 0.33 | NS |

(*continued on next page*)

**Table 3** (*continued*)

| Landmark No. | Female | | | Male | | | Gender diff. |
|---|---|---|---|---|---|---|---|
| | Mean | SD | Correlation with BMI | Mean | SD | Correlation with BMI | |
| 52 | 267.52 | 91.22 | −0.08 | 381.45 | 153.47 | 0.17 | P < 0.01 |
| 53 | 310.51 | 179.08 | 0.13 | 382.32 | 120.21 | 0.42 | NS |
| 54 | 334.01 | 171.39 | 0.05 | 396.26 | 135.14 | 0.23 | NS |
| 55 | 258.41 | 110.27 | 0.04 | 359.55 | 128.27 | 0.08 | P < 0.05 |
| 56 | 329.36 | 175.71 | 0.18 | 372.13 | 120.96 | 0.33 | NS |
| 57 | 291.08 | 128.31 | 0.13 | 382.25 | 111.46 | 0.41 | P < 0.05 |
| 58 | 285.80 | 115.97 | −0.07 | 354.46 | 145.36 | 0.39 | NS |
| 59 | 293.18 | 139.32 | −0.02 | 396.42 | 163.98 | 0.27 | P < 0.05 |
| 60 | 264.39 | 116.47 | −0.03 | 321.34 | 106.73 | 0.26 | NS |
| 61 | 267.64 | 120.89 | −0.02 | 379.14 | 150.15 | 0.32 | P < 0.05 |
| 62 | 376.62 | 173.70 | 0.01 | 531.85 | 167.19 | .55* | P < 0.05 |
| 63 | 364.01 | 162.04 | 0.10 | 471.18 | 209.77 | 0.40 | NS |
| 64 | 322.17 | 137.63 | 0.22 | 479.70 | 178.05 | 0.38 | P < 0.01 |
| 65 | 284.71 | 106.90 | −0.09 | 368.47 | 146.31 | 0.21 | P < 0.05 |
| 66 | 341.27 | 188.99 | 0.12 | 400.32 | 131.02 | 0.26 | NS |
| 67 | 352.42 | 153.28 | 0.03 | 466.08 | 148.04 | 0.22 | P < 0.05 |
| 68 | 375.16 | 170.41 | 0.03 | 438.85 | 142.79 | 0.27 | NS |
| 69 | 346.75 | 211.63 | 0.07 | 384.00 | 114.94 | 0.11 | NS |
| 70 | 293.57 | 168.88 | 0.04 | 379.22 | 129.77 | 0.35 | NS |
| 71 | 299.62 | 178.06 | 0.02 | 418.23 | 160.77 | 0.09 | P < 0.05 |
| 72 | 300.19 | 142.70 | 0.04 | 385.11 | 130.96 | 0.25 | NS |
| 73 | 257.13 | 98.17 | 0.01 | 334.47 | 137.90 | 0.33 | P < 0.05 |
| 74 | 331.02 | 152.96 | 0.04 | 433.76 | 151.57 | 0.35 | P < 0.05 |
| 75 | 362.99 | 149.89 | −0.14 | 448.81 | 142.40 | 0.18 | NS |
| 76 | 412.36 | 236.13 | 0.10 | 459.87 | 149.07 | 0.36 | NS |
| 77 | 331.02 | 189.20 | 0.24 | 392.52 | 142.89 | 0.18 | NS |
| 78 | 333.50 | 151.83 | 0.04 | 406.77 | 155.53 | 0.29 | NS |
| 79 | 354.97 | 167.00 | 0.05 | 443.71 | 139.66 | 0.42 | NS |
| 80 | 300.13 | 136.44 | 0.18 | 433.36 | 165.15 | 0.30 | P < 0.05 |
| 81 | 391.40 | 147.10 | 0.02 | 513.77 | 186.01 | 0.39 | P < 0.05 |
| 82 | 380.13 | 203.00 | 0.21 | 496.02 | 138.47 | .52* | P < 0.05 |
| 83 | 282.36 | 139.42 | 0.09 | 414.81 | 209.92 | .53* | P < 0.05 |
| 84 | 282.68 | 150.56 | 0.16 | 404.70 | 180.89 | 0.41 | P < 0.05 |
| 85 | 311.21 | 158.70 | −0.01 | 429.30 | 191.02 | .50* | P < 0.05 |
| 86 | 278.66 | 189.34 | 0.20 | 400.80 | 161.68 | 0.21 | P < 0.05 |
| 87 | 237.83 | 117.25 | −0.06 | 442.75 | 170.30 | 0.46 | P < 0.01 |
| 88 | 278.47 | 153.69 | 0.09 | 477.71 | 186.64 | .50* | P < 0.01 |
| 89 | 295.61 | 167.26 | 0.07 | 414.17 | 150.31 | 0.40 | P < 0.05 |
| 90 | 231.08 | 111.98 | −0.09 | 319.82 | 138.04 | .53* | P < 0.05 |
| 91 | 209.75 | 110.73 | 0.17 | 265.21 | 94.50 | .49* | NS |
| 92 | 187.01 | 109.03 | 0.24 | 247.61 | 97.09 | .53* | NS |
| 93 | 152.42 | 86.04 | 0.08 | 202.15 | 86.47 | 0.42 | NS |
| 94 | 164.65 | 88.76 | 0.03 | 203.66 | 88.64 | .52* | NS |
| 95 | 207.71 | 108.39 | 0.08 | 310.27 | 108.69 | .58* | P < 0.01 |
| 96 | 134.46 | 58.71 | 0.12 | 219.03 | 96.37 | 0.41 | P < 0.01 |
| 97 | 189.55 | 93.00 | 0.16 | 224.20 | 97.26 | 0.46 | NS |
| 98 | 202.74 | 98.59 | −0.04 | 279.78 | 106.14 | .63** | P < 0.05 |
| 99 | 230.19 | 91.46 | −0.03 | 294.43 | 148.88 | .57* | NS |
| 100 | 237.83 | 129.31 | 0.19 | 353.82 | 124.42 | 0.44 | P < 0.05 |
| 101 | 234.27 | 122.96 | 0.05 | 309.24 | 115.97 | .55* | NS |
| 102 | 280.96 | 143.45 | −0.09 | 413.93 | 165.15 | .65** | P < 0.05 |
| 103 | 193.95 | 81.64 | −0.13 | 311.39 | 115.23 | 0.23 | P < 0.01 |
| 104 | 165.41 | 97.37 | −0.07 | 224.44 | 105.68 | 0.43 | NS |
| 105 | 139.30 | 98.66 | 0.17 | 187.66 | 62.82 | 0.33 | NS |
| 106 | 132.23 | 83.77 | 0.05 | 173.73 | 72.07 | 0.48 | NS |
| 107 | 138.73 | 60.47 | −0.06 | 154.14 | 70.54 | .51* | NS |
| 108 | 130.51 | 66.77 | −0.01 | 179.78 | 64.44 | .62* | P < 0.05 |
| 109 | 121.53 | 76.44 | −0.23 | 144.82 | 93.65 | 0.28 | NS |
| 110 | 123.06 | 56.83 | 0.12 | 158.12 | 67.47 | 0.44 | NS |
| 111 | 108.66 | 51.61 | −0.12 | 134.24 | 84.02 | 0.38 | NS |
| 112 | 106.18 | 58.67 | −0.05 | 137.82 | 75.62 | .68** | NS |
| 113 | 155.99 | 66.24 | −0.08 | 263.69 | 98.44 | 0.29 | P < 0.01 |
| 114 | 96.05 | 42.69 | −0.22 | 133.04 | 67.65 | .59* | P < 0.05 |
| 115 | 90.19 | 46.97 | 0.16 | 121.02 | 56.20 | 0.46 | NS |
| 116 | 437.32 | 190.44 | 0.13 | 491.72 | 164.90 | .50* | NS |
| 117 | 394.33 | 223.21 | 0.22 | 485.67 | 143.01 | 0.47 | NS |
| 118 | 301.40 | 137.83 | 0.12 | 410.75 | 132.02 | 0.29 | P < 0.05 |
| 119 | 379.17 | 185.01 | 0.02 | 377.71 | 191.81 | 0.09 | NS |

## References


Álvarez-Méndez, A.M., et al., 2017. Systematic mapping of pressure pain thresholds of the masseter and temporalis muscles and assessment of their diversity through the novel application of entropy. J. Oral Facial Pain Headache 31 (4).

Barón, J., et al., 2017. Differences in topographical pressure pain sensitivity maps of the scalp between patients with migraine and healthy controls. Headache J. Head Face Pain 57 (2), 226–235.

Binderup, A.T., Arendt-Nielsen, L., Madeleine, P., 2010. Pressure pain sensitivity maps of the neck-shoulder and the low back regions in men and women. BMC Muscoskel. Disord. 11 (1), 1–7.

Brigida, L.D., et al., 2021. Discomfort threshold evaluation for hand and elbow regions: a basis for hand-held device design. In: International Conference on Applied Human Factors and Ergonomics. Springer.

Broekhuizen, R., et al., 2018. Head sensitivity for designing bicycle helmets with improved physical comfort. In: International Conference on Applied Human Factors and Ergonomics. Springer.

Bulut, O., Sipahioglu, S., Hekimoglu, B., 2014. Facial soft tissue thickness database for craniofacial reconstruction in the Turkish adult population. Forensic Sci. Int. 242, 44–61.

Buso, A., Shitoot, N., 2019. Sensitivity of the foot in the flat and toe off positions. Appl. Ergon. 76, 57–63.

Castien, R.F., et al., 2021. High concurrent validity between digital and analogue algometers to measure pressure pain thresholds in healthy participants and people with migraine: a cross-sectional study. J. Headache Pain 22 (1), 1–12.

Cha, K.-S., 2013. Soft-tissue thickness of South Korean adults with normal facial profiles. Korean J. Orthodontics 43 (4), 178–185.

Chen, F., et al., 2011. Age and sex related measurement of craniofacial soft tissue thickness and nasal profile in the Chinese population. Forensic Sci. Int. 212 (1–3), 272 e1–e6.

Chopra, K., et al., 2015. A comprehensive examination of topographic thickness of skin in the human face. Aesthetic Surg. J. 35 (8), 1007–1013.

Chung, S.-C., Um, B.-Y., Kim, H.-S., 1992. Evaluation of pressure pain threshold in head and neck muscles by electronic algometer: intrarater and interrater reliability. CRANIO® 10 (1), 28–34.

Corniani, G., Saal, H.P., 2020. Tactile innervation densities across the whole body. J. Neurophysiol. 124 (4), 1229–1240.

De Greef, S., Willems, G., 2005. Three-dimensional cranio-facial reconstruction in forensic identification: latest progress and new tendencies in the 21st century. J. Forensic Sci. 50 (1). JFS2004117-6.

Dueñas, L., et al., 2021. Influence of age, gender and obesity on pressure discomfort threshold of the foot: a cross-sectional study. Clin. BioMech. 82, 105252.

Ferreira, J., Matias, B., Silva, A.G., 2020. Pressure pain thresholds in university students with undertreated neck pain: comparison with asymptomatic individuals, reliability and measurement error. Eur. J. Physiotherp. 22 (5), 284–289.

Fredriksson, L., Alstergren, P., Kopp, S., 2000. Absolute and relative facial pressure-pain thresholds in healthy individuals. J. Orofac. Pain 14 (2).

He, R., et al., 2021. Age-and sex-related measurements of total craniofacial soft tissue thickness and fat in a central Chinese population. J. Craniofac. Surg. 32 (8), 2626–2630.

Jayaseelan, D.J., Cole, K.R., Courtney, C.A., 2021. Hand-held dynamometer to measure pressure pain thresholds: a double-blinded reliability and validity study. Musculoskelet. Sci. Pract. 51, 102268.

Johansson, R.S., Westling, G., 1984. Roles of glabrous skin receptors and sensorimotor memory in automatic control of precision grip when lifting rougher or more slippery objects. Exp. Brain Res. 56 (3), 550–564.

Kaas, J.H., et al., 1979. Multiple representations of the body within the primary somatosensory cortex of primates. Science 204 (4392), 521–523.

Kosek, E., Ekholm, J.a., Nordemar, R., 1993. A comparison of pressure pain thresholds in different tissues and body regions. Long-term reliability of pressure algometry in healthy volunteers. Scand. J. Rehabil. Med. 25 (3), 117–124.

Lacko, D., et al., 2015. Evaluation of an anthropometric shape model of the human scalp. Appl. Ergon. 48, 70–85.

Le Johansson, L., et al., 1999. Perception of surface pressure applied to the hand. Ergonomics 42 (10), 1274–1282.

Lei, Z., Yang, J., Zhuang, Z., 2012. Headform and N95 filtering facepiece respirator interaction: contact pressure simulation and validation. J. Occup. Environ. Hyg. 9 (1), 46–58.

Marshall, W.H., Woolsey, C.N., Bard, P., 1937. Cortical representation of tactile sensibility as indicated by cortical potentials. Science 85 (2207), 388–390.

Nasir, S.H., et al., 2019. Assessing the pressure and thermal discomfort thresholds for designing of therapeutic gloves: a pilot study. OBM Integrat. Complement. Med. 4 (3), 1-1.

Páris, C., et al., 2017. Bitalino use and aplications for health, education, home automation and industry. In: Proceedings of the 8th International Conference on Society and Information Technologies. IC-SIT).

Prushansky, T., Dvir, Z., Defrin-Assa, R., 2004. Reproducibility indices applied to cervical pressure pain threshold measurements in healthy subjects. Clin. J. Pain 20 (5), 341–347.

Sahni, D., et al., 2008. Facial soft tissue thickness in northwest Indian adults. Forensic Sci. Int. 176 (2–3), 137–146.

Sand, T., et al., 1997. The reproducibility of cephalic pain pressure thresholds in control subjects and headache patients. Cephalalgia 17 (7), 748–755.

Sarilita, E., et al., 2020. Facial average soft tissue depth variation based on skeletal classes in Indonesian adult population: a retrospective lateral cephalometric study. Leg. Med. 43, 101665.

Shah, P., Luximon, Y., 2021. Assessment of pressure sensitivity in the head region for Chinese adults. Appl. Ergon. 97, 103548.

Shah, P., Luximon, Y., Luximon, A., 2017. Use of soft tissue properties for ergonomic product design. In: International Conference on Applied Human Factors and Ergonomics. Springer.

Shah, P., Luximon, Y., Luximon, A., 2022. Measurement of soft tissue deformation at discomfort and pain threshold in different regions of the head. Ergonomics 1–26 (just-accepted).

Spano, V.E., et al., 2021. Increased somatosensory amplification is associated with decreased pressure pain thresholds at both trigeminal and extra-trigeminal locations in healthy individuals. J. Oral Rehabil. 48 (1), 10–17.

Stephan, C.N., Simpson, E.K., 2008. Facial soft tissue depths in craniofacial identification (part I): an analytical review of the published adult data. J. Forensic Sci. 53 (6), 1257–1272.

Tedeschi-Oliveira, S.V., et al., 2009. Facial soft tissue thickness of Brazilian adults. Forensic Sci. Int. 193 (1–3), 127 e1–e7.

Vink, P., Hallbeck, S., 2012. Editorial: comfort and discomfort studies demonstrate the need for a new model. Appl. Ergon. 43 (2), 271–276.

Vink, P., Lips, D., 2017. Sensitivity of the human back and buttocks: the missing link in comfort seat design. Appl. Ergon. 58, 287–292.

Waller, R., et al., 2016. Pressure and cold pain threshold reference values in a large, young adult, pain-free population. Scandinavian J. Pain 13 (1), 114–122.

Weerasinghe, T.W., Goonetilleke, R.S., Reischl, U., 2017. Pressure thresholds and stiffness on the plantar surface of the human foot. Ergonomics 60 (7), 985–996.

Wenxiu Yang, R.H., Chen, Tingshu, Wang, Haining, Goossens, Richard, Huysmans, Toon, 2022. Soft Tissue Thickness Estimation for Head, Face, and Neck from CT Data for Product Design Purposes. Conferences of International Association of Universities and Colleges of Art, Design and Media.

Wiggermann, N., Keyserling, W.M., 2015. Time to onset of pain: effects of magnitude and location for static pressures applied to the plantar foot. Appl. Ergon. 46, 84–90.

Xiong, S., Goonetilleke, R.S., Jiang, Z., 2011. Pressure thresholds of the human foot: measurement reliability and effects of stimulus characteristics. Ergonomics 54 (3), 282–293.

Xiong, S., et al., 2013. A model for the perception of surface pressure on human foot. Appl. Ergon. 44 (1), 1–10.

Yang, W., Wang, H., He, R., 2022. Establishment of a finite element model based on craniofacial soft tissue thickness measurements and stress analysis of medical goggles. Ergonomics 65 (2), 305–326.